Removal of adsorbing estrogenic micropollutants by nanofiltration membranes

Removal of adsorbing estrogenic micropollutants by nanofiltration membranes. Part B – Model Development

Journal of Membrane Science
2013
Volume 431, 257-266

Andrea J. C. Semião*, Matthieu Foucher, Andrea I. Schäfer
School of Engineering, The University of Edinburgh,
Edinburgh, EH9 3JL, United Kingdom

* Corresponding author: Andrea J. C. Semião, Presently at University College Dublin E-mail: Andrea.Correia-Semiao@ucd.ie

Abstract

Removal of estrone (E1) and estradiol (E2) by nanofiltration membranes at neutral pH is carried out both by size exclusion and adsorption. Size exclusion is dependent on the solute to pore radius ratio and the hormone-membrane affinity. It has been shown that the higher the affinity between the trace contaminant and the membrane active layer, the more will partition and penetrate inside the membrane and in consequence permeate. Adsorption, on the other hand is dependent on the hormone concentration, the adsorption isotherm constant (i.e. proportion between the equilibrium concentration and the mass adsorbed) and membrane area available for sorption.

To establish the transport mechanisms involved in the removal of trace contaminants by NF membranes, it is essential to discern between the different contributions of each of these effects independently. In reality, NF membranes have different pore radius, internal surface area and affinity with the contaminants, of which most of these are difficult to determine.

This paper developed for the first time a model that describes the transport of hormones E1 and E2 through the NF membrane pores, in this case the NF 270 membrane, by taking transient adsorption into account. The different mechanisms of size exclusion, adsorption and membrane affinity were considered by modifying the hydrodynamic model.

The model was numerically solved and allowed to obtain the concentration profiles along the NF270 membrane pore as a function of time. The model was validated by integrating these profiles and determining the total mass adsorbed on the membrane in transient regime that was then compared to the experimental data.

Despite E1 adsorbing 20% more mass than E2 in static mode for the NF 270 membrane (i.e. no pressure applied), E1 adsorbs twice as much as E2 under the same cross-flow conditions. The much higher adsorption obtained for E1 in filtration mode can be explained by a higher partitioning inside the membrane, compared to E2. A higher partitioning increases the concentration of E1 inside the membrane pore, and as a consequence, causes higher adsorption. The model developed allowed therefore to clearly distinguish between the contributions of the different mechanisms involved in the removal of adsorbing hormones through NF membranes, i.e. concentration polarisation, solute-membrane affinity, size exclusion, adsorption, diffusion and convection. Although much debate exists on whether solute transport in NF pores is carried out solely by diffusion or by diffusion-convection, this model showed that transport by convection and diffusion described well the transport of adsorbing hormones by NF membranes, where convection especially contributed to the hormone transport for pressures above 11 bar.

Keywords: trace contaminant transport, nanofiltration, adsorption, convection, diffusion

1 Introduction

Hormones have been found at concentrations up to 76 $ng.L^{-1}$ and 2 $\mu g.L^{-1}$ in sewage treatment plant and agricultural effluents, respectively [1, 2]. These effluents are discharged in surface waters (*e.g.* rivers) where concentrations of hormones in the $ng.L^{-1}$ level have been measured [3]. For example, in some rivers in the US up to 800 $ng.L^{-1}$ have been measured in streams [4]. Since they pose an environmental and potential health risk to organisms [5], such contaminants should be removed from natural and potable water sources. Nanofiltration (NF) is a possible treatment solution.

Transport mechanisms and retention of ions and some neutral organic solutes by NF membranes are generally well understood [6-8]. Pollutants larger than the membrane pore size are expected to be retained because of a sieving effect [9-11]. Van der Bruggen *et al.* [10] showed that molecular weight (MW) is a good indicator of NF and RO retention compared to other molecular sizes such as Stokes diameter.

In consequence, NF membranes are expected to effectively remove hormones of molecular weight greater than 270 $g.mol^{-1}$. However, hormone observed retention varies greatly (from <10% up to 100%) [12]. This can be attributed to either different filtration conditions (*e.g.* pressure) [13] or to enhanced partitioning inside the membrane pore [14] which results in a lower performance than would be expected solely by size exclusion [15, 16].

Furthermore, the occurrence of hormone adsorption onto the membranes is well documented [17, 18]. The accumulation of contaminants on the polymeric membranes poses a risk since the contaminants can desorb from the membrane during operation or cleaning and contaminate the permeate [19-21]. In order to avoid the occurrence of adsorption it is necessary to understand what parameters affect adsorption and which mechanisms control the process. Retention of adsorbing compounds has been shown to be enhanced when their adsorption is decreased due to preferential adsorption of another contaminant on the membrane [22], showing a link between adsorption and retention.

The principal component analysis method (quantitative structure relations (QSR)) has been used to describe retention of trace contaminants by NF membranes as a function of (1) the contaminants properties (*e.g.* molecular width and depth) [23, 24] and (2) the membrane characteristics (*e.g.* roughness and active layer thickness) [11]. Other studies modelling the retention of adsorbing trace contaminants with the hydrodynamic model combined the effect of steric exclusion and contaminant-membrane affinity in the partitioning on the nanofiltration

membrane pore [14, 25, 26]. The modified model predicted the contaminant retention with permeate flux very well. However, these previous studies were carried out after membrane saturation had been reached, and no insight on the adsorption mechanisms was provided. The mechanisms governing the adsorption and its effect in adsorbing trace contaminant transport onto NF membranes are not well understood, and the inclusion of an adsorption term into retention models is to date lacking.

The occurrence of adsorption has presented a new challenge in the retention modelling of adsorbing contaminants in NF membranes. Firstly, in some cases, a continuous adsorption of the contaminant on the membrane prevented the application of steady-state retention models developed [25, 27] because the permeate concentration was not detectable. Secondly, the addition of a transient adsorption term in the transport equation increases considerably the complexity of the process.

Adsorption has been considered in a modified sorption-diffusion model for RO that added adsorption induced flux decline to pressure [28]. This model predicted well the permeate concentration. However, it did not consider a convection element, which might be expected to occur in NF. Furthermore it took into account a flux reduction element caused by sorption of the trace contaminant onto the membrane [29]. A flux decrease, however, does not always occur, possibly due to the low concentrations used ($<\mu g.L^{-1}$) [13, 22, 28]. The addition of a convection term in combination with a transient term for adsorption into the contaminant mass transport considerably increases the problem complexity.

Membrane pore radius as well as the surface and internal area were experimentally found to have an effect on adsorption, as shown in Part A of this paper. The bigger the pore radius and the more internal surface area a membrane has, the more contaminant will adsorb. This indicates that a relation between the solute and pore radius, as well as the internal membrane area need to be taken into account when modelling trace contaminant adsorption onto NF membranes.

Contaminant-membrane affinity [14] further needs to be taken into account. The trace contaminant partitions to the polyamide active layer and causes a lower retention than would be expected [30]. It is however difficult to distinguish experimentally between the different contributions of each of these previous effects: pore radius, internal area, adsorption and contaminant-membrane affinity since they are all at play during filtration. Furthermore, NF membranes have different pore radius distributions, adsorption capacity, immeasurable internal surface area and hormone-polymer affinity.

To overcome those short-falls, a transport model that takes adsorption into account was developed. The hydrodynamic model was modified by taking into account steric exclusion, adsorption and hormone-membrane affinity. This model has been successfully used to describe the

transport of solutes by NF membranes [7, 14]. The model allows two things: firstly understanding how the different membrane characteristics such as pore radius, internal surface area and partitioning influence adsorption, which is valuable information for the design of new non-adsorbing membranes; secondly it allows understanding how the mechanisms of diffusion, convection and adsorption may contribute to the transport of hormones by NF membranes. The concentration profile of the hormone along the membrane thickness is obtained while adsorption occurs, allowing elucidating which transport mechanisms are involved. Integrating the transient concentration profile along the pore allows obtaining the transient mass adsorbed. The model predictions are consistent with the experimental mass adsorbed with time and was hence shown to describe well the transport of adsorbing hormones by NF membranes.

2 Theory and Model Development

2.1. Mathematical Model

The mathematical model describing the transport of adsorbing solutes through NF membranes is described next. Firstly the mathematical equation describing the transport of solutes in a membrane pore is obtained by a mass balance to a differential volume in the pore. Secondly the boundary conditions needed to solve the transport equation are determined.

2.1.1 NF Pore Transport Equation

In the Part A of this paper, it was established that the ratio solute to pore radius (r_s/r_p) and the internal available surface area of the active layer need to be taken into account in adsorption and, hence, the transport modelling of hormones in NF membranes.

The hydrodynamic model reviewed by Deen [31] was chosen as a basis to describe the transport of adsorbing hormones in NF membranes. First, this model takes into account the above-mentioned influencing parameter ratio of solute to membrane pore size (r_s/r_p). Then, by considering the membrane as having perfectly cylindrical pores with an average pore radius r_p and length δ (active layer thickness), this model allows using the internal surface area as a parameter in modelling hormone adsorption on NF pores. In reality, the membranes are known to have a distribution of pore sizes [7, 32] and the pores exhibit tortuosity. This later parameter has however never been determined or measured for NF membranes.

The solute molecule, assumed to be a spherical particle, is transported to the pore entrance where it partitions in the feed, is transported by convection and diffusion inside the pore and then

partitions on the permeate side. Figure 1 presents this mechanism schematically with the partitioning at the pore entrance (feed side) between C_{mp} and C_{mf} and the pore exit (permeate side) between C_{pp} and C_p.

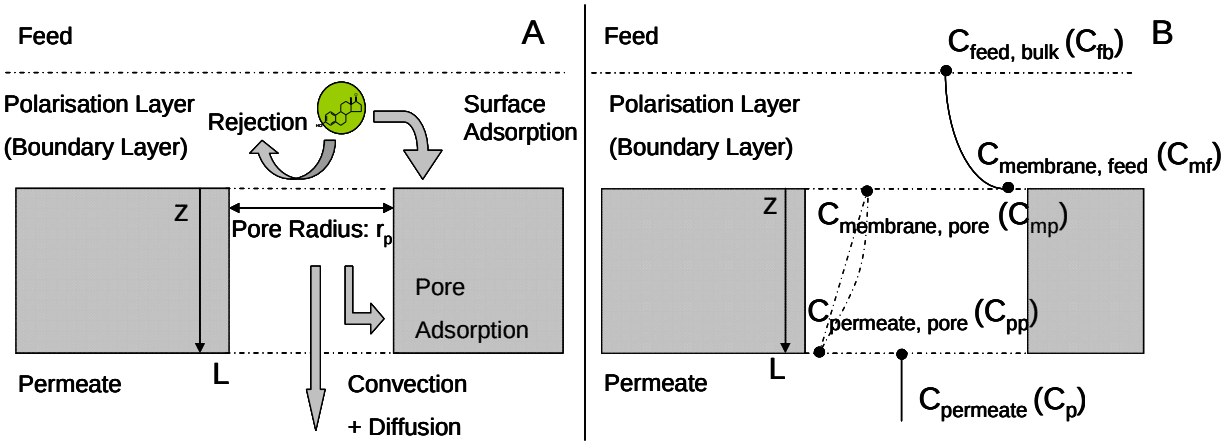

Figure 1 Physical phenomena occurring in the filtration of adsorbing compounds onto NF membrane active layer with an effective pore size

Performing a mass balance to a solute A in a differential control volume inside the membrane pore for a time interval δt and thickness δz yields equation (1):

$$-A_a \frac{\partial j_A}{\partial z} - P_p \frac{\partial \Omega}{\partial t} = A_a \frac{\partial C_A}{\partial t} \qquad (1)$$

where A_a (m^2) is the area of solute passage (corresponding to the permeation area), j_A is the solute flux ($kg.s^{-1}.m^{-2}$)), z is the membrane depth (m) from the pore entrance to the pore exit, P_p is the pore perimeter (m), Ω is the mass adsorbed per surface area ($kg.m^{-2}$), t is time (s) and C_A is the solute concentration inside the pore ($kg.m^{-3}$). In the previous equation, the first term of the left-hand side stands for the solute convective/diffusive transport inside the membrane pore, the second term accounts for the solute adsorption on the pore surface and the right-hand side term represents the accumulation rate of the solute in the pore.

The solute flux j_A may have both convective and diffusive terms [31] given by equation (2):

$$j_A = -K_d D_\infty \frac{dC_A}{dz} + K_c V C_A \qquad (2)$$

where D_∞ ($m^2.s^{-1}$) is the solute diffusion coefficient in solution, V ($m.s^{-1}$) is the radial average fluid velocity in a cylindrical pore, calculated as the permeate flux divided by the membrane porosity ε and K_c and K_d are the hindrance factors accounting for the drag caused by the pore walls on the solute.

Substituting equation (2) in equation (1) yields equation (3) which describes the solute concentration inside the pore.

$$-K_c V \frac{\partial C_A}{\partial z} + K_d D_\infty \frac{\partial^2 C_A}{\partial z^2} = \frac{\partial C_A}{\partial t} + \frac{P_p}{A_a} \frac{\partial \Omega}{\partial t} \quad (3)$$

The last term on the right-hand side of equation (3) takes into account experimental evidence where the membrane adsorption isotherm for both hormones was found to be linear [13] (equation 4).

$$\Omega = X C_A \quad (4)$$

where X is the straight line slope (m). The time variation of equation (4) is given by:

$$\frac{\partial \Omega}{\partial t} = X \frac{\partial C_A}{\partial t} \quad (5)$$

Equation (5) can be substituted into equation (3) assuming that sorption in the membrane pore surface is faster compared to the velocity in the pore, a common assumption used to model the transport of adsorbing contaminants in groundwater and porous media [33, 34]. Adsorption experiments carried out with the grinded polymer polyamide (Part A of the paper) and with the static experiments in Figure 8 showed that in the first hour of the experiment, more than 70% of the total hormone mass adsorbed occurred. This shows that the adsorption process onto the polyamide is very quick, and hence, the assumption of substituting equation (5) in equation (3) is valid. After algebraic manipulation one obtains equation (6):

$$-K_i \frac{\partial C_A}{\partial z} + D_i \frac{\partial^2 C_A}{\partial z^2} = \frac{\partial C_A}{\partial t} \quad (6)$$

where K_i and D_i are given by equation (7a) and (7b), respectively:

$$Di = \frac{K_d D_\infty}{(1 + \frac{P_p}{A_a} X)} \quad (7a)$$

$$Ki = \frac{K_c V}{(1 + \frac{P_p}{A_a} X)} \quad (7b)$$

Once the transport equation (equation 6) has been determined, the next step is to establish the boundary conditions used to solve equation (6).

2.1.2 Boundary Conditions

To solve the time dependent equation (6), an initial condition and two spatial boundary conditions are required. The initial and boundary conditions used are presented in equations (8a, b and c):

$$C_A = 0, t = 0, \forall z \quad (8a)$$

$$C_A = C_{mf} \Phi', z = 0, t>0 \quad (8b)$$

$$C_A = C_p \Phi', z=L, t>0 \quad (8c)$$

When the hormone is added to the system, in the first instance the concentration inside the membrane pore is zero (equation 8a). For the spatial boundary conditions, the concentration at the pore entrance (C_{mp} in Figure 1) is equal to the concentration at the membrane surface (C_{mf}) multiplied by the steric partitioning coefficient modified for interaction between the solute and the membrane [14]. The same spatial boundary condition is applied on the permeate side (C_{pp} and C_p).

Concentration polarisation needs to be taken into account when modelling adsorption and retention of hormones in NF membranes (equation 8b). As was shown in a previous study [13] this phenomenon causes an increase in solute concentration at the membrane surface, originating a concentration gradient from the bulk feed (C_{fb}) to the membrane surface (C_{mf}) as depicted in Figure 1. The more pronounced the polarisation is the higher C_{mf} will be. In consequence more solute will adsorb to the membrane polymer and less will be retained [13]. The boundary conditions C_{mf} and C_p

were determined with the experimental data for different conditions of filtration (*e.g.* pressure) as explained in section 4.1.2.

2.2. Numerical Model

2.2.1 Model Development

Equation (6) has been applied in the transport of contaminants through porous media [35]. To the author's knowledge, equation (6) has never been applied in nanofiltration of trace contaminants. There is no analytical solution for the unsteady-state partial differential equation (6) with the boundary conditions expressed by equations (8a, b and c). There are very particular situations that allow solving equation (6) analytically. For example, transport in porous media with adsorption expressed similarly to equation (6) can be analytically solved considering the media as infinite with a nil concentration there [35]. For the case of NF membranes with a few nanometres of thickness this approach cannot be used.

The previous reasoning leads to the conclusion that the solution of equation (6) requires a numerical method. In this work the finite difference method is applied. A grid is built to discretize the physical domain so that the dependent variables are calculated at discrete points: the grid nodes. The spatial derivative expressions are replaced by finite differences obtained by Taylor's series expansion. Both first and second derivatives are calculated by the second order central differencing scheme (equations (9a) and (9b), respectively), which has a truncation error $O(\delta z)^2$, to ensure higher results accuracy [36].

$$\left.\frac{\partial C_A}{\partial z}\right|_k = \frac{C_{A,k+1} - C_{A,k-1}}{2\delta z} + O(\delta z)^2 \qquad (9a)$$

$$\left.\frac{\partial^2 C_A}{\partial z^2}\right|_k = \frac{C_{A,k+1} - 2C_{A,k} + C_{A,k-1}}{(\delta z)^2} + O(\delta z)^2 \qquad (9b)$$

where C_A is the solute concentration, z is the entrance-exit direction inside the pore, k is a grid node with k-1 and k+1 being, respectively, the upstream and downstream neighboring grid nodes, each of them distancing δz from the node k.

The unsteady character of equation (6) (*i.e.* dependency on time) was dealt with the full implicit method, which is of first order in time $O(\delta t)$. This scheme is unconditionally stable as opposed to the explicit scheme. Therefore, no particular time step (δt) limitations are required [36].

Applying the central differencing and the full implicit schemes to equation (6) for the generic k grid node, and denoting superscripts n and n+1 as two consecutive moments separated by the time step δt, the algebraic equation (10) is obtained:

$$\frac{C_{A,k}^{n+1} - C_{A,k}^{n}}{\delta t} = D_i \frac{C_{A,k+1}^{n+1} - 2C_{A,k}^{n+1} + C_{A,k-1}^{n+1}}{(\delta z)^2} - K_i \frac{C_{A,k+1}^{n+1} - C_{A,k-1}^{n+1}}{2\delta z} \qquad (10)$$

Equation (10) must be written for each grid node, which leads to a set of n equations with n unknowns (the concentration at the nodes), n being the number of grid nodes. The first and last nodes of the grid which are inside the pore and nearest the pore entrance and exit respectively must include the boundary conditions expressed by equations (8b) and (8c), where the experimental results measured for the transient feed and permeate concentrations are used, as explained in section 4.1.2.

The set of equations is solved by a matrix algorithm in Matlab to obtain the concentration profile along the pore for different times. In the present case the tridiagonal matrix algorithm (TDMA) was used [36].

2.3. Concentration Profile and Mass Adsorbed

2.3.1 Surface Mass Adsorbed

Due to the adsorption of hormone onto the membrane, the membrane surface concentration decreases with time. The relationship between the mass adsorbed on the surface and the concentration at the membrane surface is hence given by equation (11), similarly to equation (5),

$$\frac{dM_{ads\ surface}}{dt} = A_{surface} \frac{d\Omega_{surface}}{dt} = -A_{surface} X \frac{dC_{mf}}{dt}, \qquad (11)$$

where M_{ads} surface is the hormone mass adsorbed on the surface (ng), $A_{surface}$ is the membrane surface area (cm^2), $\Omega_{surface}$ is the mass adsorbed per surface area ($ng.cm^{-2}$), t is time (s) and X is the same parameter as defined in equation (4).

Solving equation (11) with an initial boundary condition: t=0, M_{ads}=0 and C_{mf}=C_m(0) gives equation (12),

$$M_{ads\ surface} = A_{surface} X (C_{mf}(0) - C_{mf}(t)) \qquad (12)$$

where $C_{mf}(0)$ is the concentration at the membrane surface for t=0 and $C_{mf}(t)$ is the concentration at the membrane surface for t>0 (section 4.1.2).

The concentration profile inside the membrane pores can hence be obtained, as explained next.

2.3.2 Pore Mass Adsorbed and Model Prediction Results Comparison with Experimental Data

The hormone concentration profile inside the pore is obtained by solving numerically equation (6) with the boundary conditions expressed by equations (8a, b and c).

Once the pore concentration profile is obtained, the pore mass adsorbed is estimated by numerically integrating the concentration profile along the pore and considering the linear relationship given by equation (4). The pore mass adsorbed is then summed to the surface mass adsorbed for each time, given by equation (12) and compared to the experimental results obtained for each hormone and each filtration condition.

3 Experimental Methods and Materials

The following section describes the hormone adsorption filtration experiments carried out to solve the previously described model, along with experimentally determined parameters needed for the model such as the hormone-membrane affinity constant Φ'.

3.1. Cross-Flow System

The stainless steel cross-flow system used for the filtration experiments has been described elsewhere [12]. The system is connected to a flat sheet membrane cell (MMS, Switzerland) of 46 cm^2 surface area, with a slit type channel height of 1×10^{-3} m, width of 0.025 m and length of 0.191 m.

3.2. Membrane and Membrane Characteristics

The NF270 membrane was used in this study (FilmTec Corp., MN, USA). It is a thin-film composite (TFC) membrane consisting of a polyamide active layer with polysulfone and polyester support layers and a very low surface roughness. Membrane characteristics can be found in Table 1.

Table 1 NF 270 membrane characteristics [13]

Isoelectric Point	Water Permeability ($L.h^{-1}.m^{-2}.bar^{-1}$)	NaCl Rejection (%) (0.1 M, 10 bar)	MWCO (Da)	Roughness R_A (nm)
pH 3.6	17.0 ± 0.8	52 ± 3	180 ± 20	4.2 ± 0.3

3.3. Chemicals and Reagents

The radiolabelled hormones used were [2,4,6,7-^{3}H] estrone (E1) and [2,4,6,7-^{3}H] 17β-estradiol (E2) (Perkin Elmer and GE Healthcare, UK). An initial hormone feed concentration of 100 $ng.L^{-1}$ was used in all the experiments, unless otherwise stated. A volume of 0.5 mL of sample was placed in a scintillation vial (Perkin Elmer, UK) with 4 mL of Ultima Gold LLT (Perkin Elmer, UK) and counted for 10 minutes each using a Beckman LS 6500 scintillation counter (Fullerton, USA). The detection limit of this method is 1 $ng.L^{-1}$ ± 2% for the hormones studied.

3.4. Hormone Filtration Protocol

The membrane coupon, washed and stored in MilliQ water for at least 12 hours, was placed in the cross-flow cell and compacted for two hours with MilliQ water at 25 bar. The pure water flux was measured at 25 bar for at least 30 minutes to ensure steady flux followed by flux measurement at the experimental pressure for ten minutes. The system was then emptied and replenished with 1.5 L of fresh MilliQ water, which is recirculated in the system for one hour at a set hydrodynamic condition of pressure (3 to 17 bar) and feed flow rate Q_{feed} (0.5 to 2 $L.min^{-1}$) to ensure all process parameters were constant.

A volume of 0.5 L of hormone solution was then added to the 1.5 L of circulating MilliQ water to reach the required hormone concentration in the system and mixed well using a mechanical stirrer at 200 rpm (Gallenkamp). The feed and permeate hormone concentrations were measured at regular time intervals (every five minutes for the first half hour and then once every hour) to obtain the transient trend until equilibrium was reached (average of 8 hours). The transient mass adsorbed was then obtained by mass balance to the feed tank. A new membrane was used for every experiment.

Estrone adsorption on the membrane surface in the cross-flow system was determined by circulating a solution of 100 ng.L^{-1} initial concentration without production of permeate flux, *i.e.* no pressure applied. The retentate was recirculated back to the feed tank and hormone adsorption on the membrane surface was obtained by mass balance.

3.5. Partition Coefficient Φ' Determination

The partition coefficient for each hormone E1 and E2 and the NF 270 membrane was determined by pre-saturating a membrane at 11 bar, with an initial hormone feed concentration of 50 ng.L^{-1} and a feed flow rate of 2 L.min^{-1} (Re_h=1450) to avoid polarisation. According to the literature the transitional Re_h for slit channels with hydrodynamically smooth walls varies between 1150 and 1450 [37-39]. The hormone feed and permeate concentration were then measured for several pressures, or permeate fluxes, after an hour equilibration for each pressure.

3.6. Static Adsorption Isotherms

Hormone static adsorption (no pressure) onto the NF 270 membrane was carried out in a shaker. A membrane area of 2 cm^2 was gently washed with MilliQ water, placed in 60 mL of E1 and E2 solutions of different concentrations (25, 50, 100 and 200 ng.L^{-1}) and shaked in a Certomat BS-1 UHK-25 shaker (Göttingen, Germany) for at least 48 hours at 200 rpm and 25ºC.

4 Results and Discussion

4.1. Model Coefficients

The solution of equation (6) requires several membrane and solute characteristics. Firstly, the NF membrane characteristics need to be determined in order to model the transport of the hormone through the pore. These characteristics include the average pore radius, the porosity and the active layer thickness. Secondly, the hormone characteristics also need to be determined such as the hormone diffusivity and Stokes radius. Thirdly, the affinity partition coefficient between the hormone and the active layer as well as the concentration at the membrane surface for the boundary conditions (8a) to (8c) need to be determined. Finally the proportion between the concentration in the liquid and the mass adsorbed on the membrane of equation (4) and (5) also need to be determined, as explained in the next sections.

4.1.1 Membrane and Solute Characteristics

The membrane characteristics, such as active layer thickness and pore radius, needed to solve equation (6) were estimated in the first part of this paper (part A) and are summarized in Table 2.

Table 2 NF 270 membrane active layer characteristics: average pore radius, active layer thickness to porosity ratio, effective interfacial area and porosity

Average Active Layer Thickness (nm)	**Average Pore Radius r_p (nm)**	**Active Layer Thickness Porosity Ratio δ/ε (µm)**	**Effective Interfacial Area of Active Layer A_{total} (cm^2) per 46 cm^2 of membrane**	**Porosity**
21 ± 2.4	0.42 ± 0.02	1.10 ± 0.04	134 ± 18	0.020 ± 0.002

The hormones diffusivity were calculated using the Worch equation [40] and the equivalent sphere solute radius was estimated using the Stokes-Einstein equation [31]. The results for estrone (E1) and estradiol (E2) are presented in Table 3.

Table 3 Hormones E1 and E2 properties (for further properties on the hormones refer to Schäfer *et al.* [12])

Hormone	**D_∞ ($m^2.s^{-1}$)**	**r_s (nm)**
estrone E1	5.87×10^{-10}	0.396
17-β-estradiol E2	5.85×10^{-10}	0.402

4.1.2 Concentration at the Membrane Surface Determination

The transient concentration at the membrane surface, C_{mf}, is calculated with the concentration polarisation and film theory [13] using the experimental transient feed and permeate concentrations presented in a previous study [13] for the pressures 5 bar and 8 bar (Re_h=427) and

Re_h numbers of 570, 855 and 998 (P=11 bar). For the pressure at 15 bar, the experimental results are presented in Figure 2.

The mass transfer coefficient k, necessary to calculate C_{mf} is obtained from a Sherwood correlation for the same hydrodynamic conditions [41].

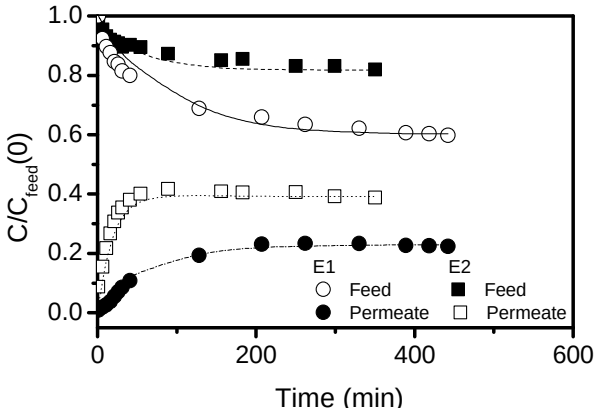

Figure 2 E1 and E2 experimental dimensionless feed and permeate concentration at 15 bar and the NF 270 ($C_{feed\ initial\ (t=0)}$=100 ng.L^{-1}, T=24°C, pH 7, Re_h=427)

4.1.3 Determination of the proportion between mass adsorbed and concentration X

The parameter X in equations (4), (7a) and (7b) needs to be determined so that the solution of equation (6) can be obtained. Each pair solute-membrane has its own X value. The parameter X gives a direct proportion between the hormones mass adsorbed subjected to a homogeneous and known concentration for a specific surface area. This parameter, however, cannot be directly obtained from the slope of the filtration isotherm experiments because the membrane is not subjected to a single concentration, but to a range of concentrations: the membrane surface concentration and the concentrations inside the pore. The parameter X was hence determined by fitting equation (6) to the filtration experiments of varying hormone feed concentration.

The fitting results for E1 and E2 are shown in Figure 3. The values obtained are: $X_{NF\ 270\text{-}E1}$=0.21 ± 0.02 m and $X_{NF\ 270\text{-}E2}$=0.17 ± 0.02 m. As expected, the value obtained for E1 is higher than the one obtained for E2, since E2 is found to adsorb less than E1 [13].

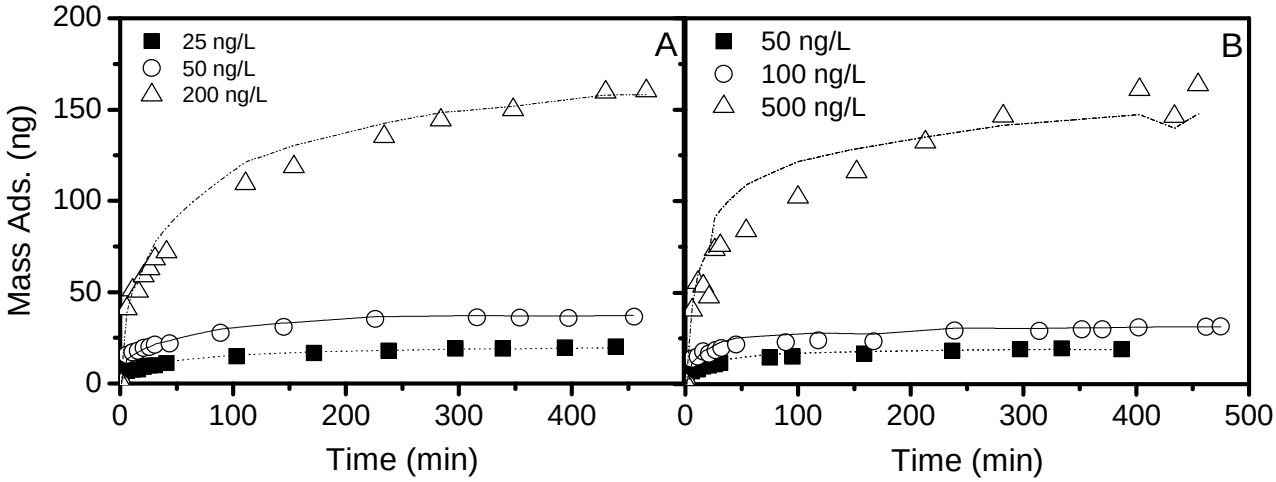

Figure 3 Model fitting to feed concentration experiments for (A) E1 and (B) E2 ($C_{feed\ E1}$=25, 50 and 200 ng.L^{-1}, $C_{feed\ E2}$=50, 100 and 500 ng^{-1} P=11 bar, Re_h=427, T=24°C, pH=7)

4.1.4 Partition Coefficient

The parameter Φ' (equation 13) needs to be determined in order to solve equation (6) with the boundary conditions (8a) and (8b) and obtain the concentration profile along the membrane pore for a solute that interacts with the membrane polymer. Partitioning at the membrane entrance and exit cannot be considered as purely sterical [31] since the hormone interacts with the membrane.

The parameter Φ' is given by equation (13),

$$\Phi' = \frac{C_{mp}}{C_{mf}} = \frac{C_{pp}}{C_p} = (1-\lambda)^2 \exp\left(-\frac{\Delta G_i}{kT}\right) = \Phi\ B \qquad (13)$$

where $\lambda = r_s/r_p$, r_s and r_p being the solute and pore radius respectively, k is the Boltzman constant, T is the temperature (K) and ΔG_i is the Gibbs energy of interaction between the solute and the membrane in the water phase.

The parameter Φ' is determined by fitting the hydrodynamic model with the modified partition coefficient Φ' to the experimental results of the hormone real retention as a function of the permeate flux [14]. Retention is determined for a pre-saturated membrane, to avoid contribution of adsorption in the removal mechanism, and at conditions of minimum concentration polarisation. Results are presented in Figure 4. The results obtained for the constant B were 35.0 for E1 and 38.4 for E2.

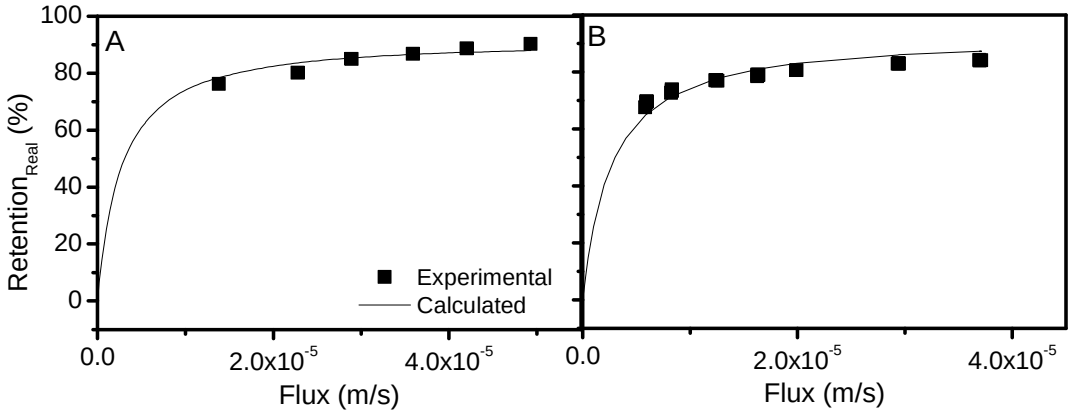

Figure 4 Determination of the solute-affinity constant B for (A) E1 and (B) E2 and NF 270 membrane (C_{feed}=50 ng.L^{-1}, Re_h=1450, T=24°C)

4.2. Numerical Model Convergence

The steady-state version of equation (6) has the following analytical solution (*i.e.* no occurrence of adsorption):

$$C_A(z) = \Phi' C_{mf} e^{\frac{Ki}{Di}z} - \frac{\Phi' C_p - \Phi' C_{mf} e^{\frac{Ki}{Di}L}}{1 - e^{\frac{Ki}{Di}L}} e^{\frac{Ki}{Di}z} + \frac{\Phi' C_p - \Phi' C_{mf} e^{\frac{Ki}{Di}L}}{1 - e^{\frac{Ki}{Di}L}} \qquad (14)$$

To verify if the numerical model with adsorption describes well the problem one can compare the results obtained by the adsorption numerical model at equilibrium conditions given by equation 6 (numerical model with adsorption at steady-state, Num. Ads. at Steady-State in Figure 5) with the analytical solution given by equation (14). As can be seen in Figure 5, that exhibits such comparison, they coincide showing the good accuracy of the solution of the numerical model.

Moreover, tests of grid independence showed that a grid comprising of more than 100 nodes was found sufficient for the solution to be grid independent with an error below 10^{-6} ng.L^{-1}.

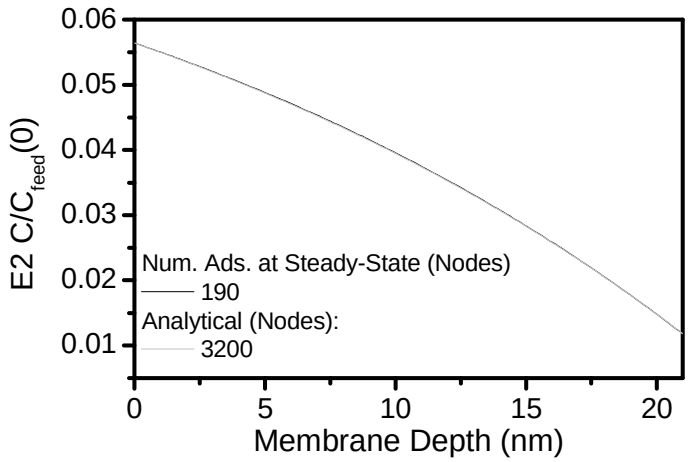

Figure 5 Comparison between the analytical solution and the numerical solutions with different grid sizes for no adsorption and the numerical model with adsorption once steady-state is reached (5 bar, 100 ng.L^{-1} E2, Re_h=427 and at equilibrium conditions)

4.3. Pore Concentration Profiles

The predicted pore concentration profiles obtained from the model clarify the dominating transport mechanisms inside the NF membrane pore.

Figure 6 A and B exhibit the transient concentration profiles for E1 at pressures of 5 and 15 bar. Figure 6 E and F shows the same results for E2. For comparison purposes, Figure 6 C and G show the concentration profiles of E1 and E2, respectively, that would be obtained at 5 bar if no adsorption occurred. Figure 6 D and H show the concentration profiles that would be obtained at 15 bar if no adsorption occurred. The boundary conditions used in this later case were the ones obtained experimentally when adsorption occurs, *i.e.* they are the same as the ones used in Figure 6 A, B, E and F.

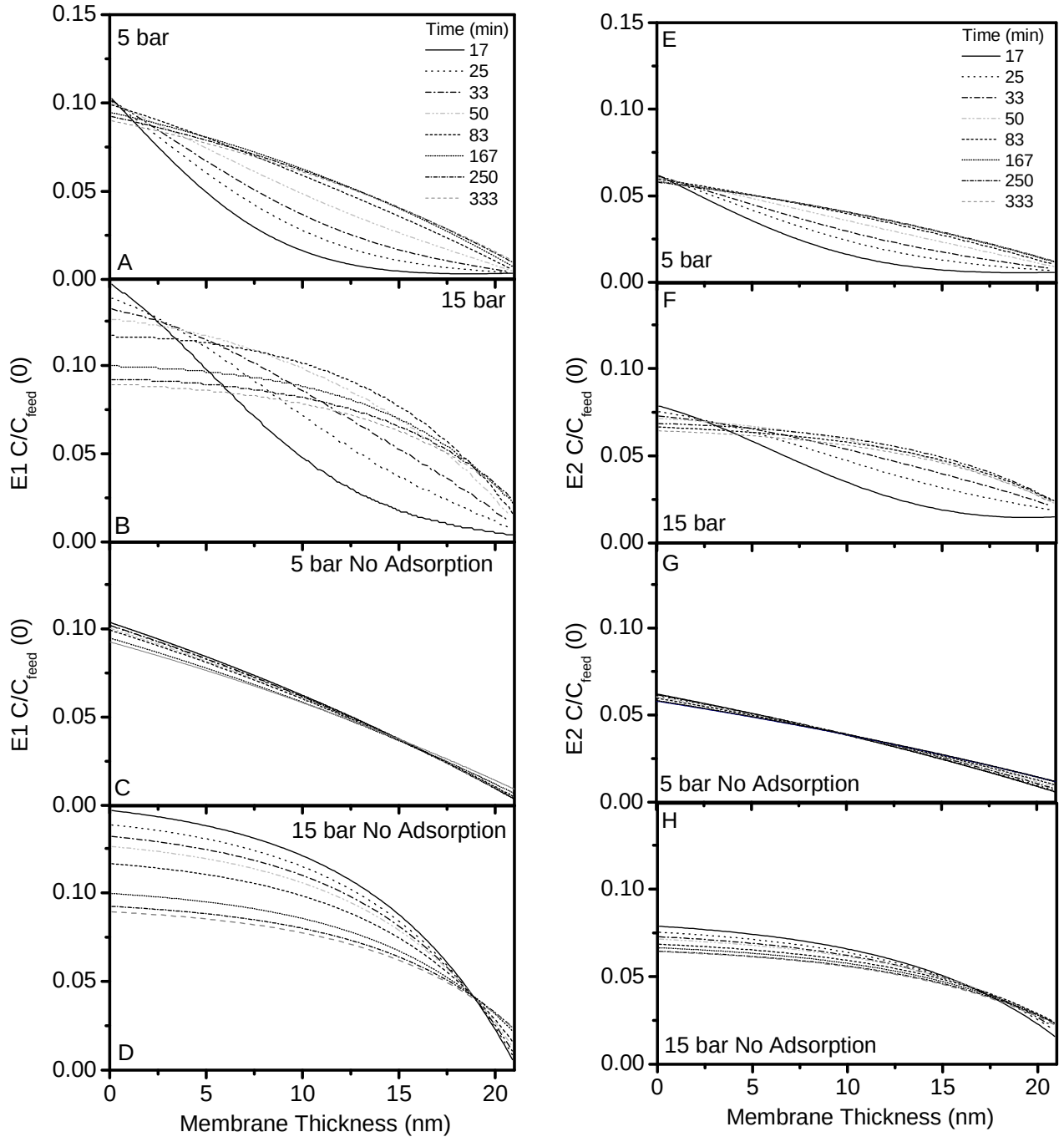

Figure 6 Modelled pore concentration profiles for E2 and E1 as a function of time (Re_h=427; C_{feed} =100 ng.L^{-1}); E2: A) 5 bar, B) 15 bar with adsorption and C) 5 bar and D) 15 bar with no adsorption; E1: E) 5 bar, F) 15 bar with adsorption and G) 5 bar and H) 15 bar with no adsorption

Comparing Figure 6 A with C and B with D for E1 (or Figure 6 E with G and F with H for E2), the effect of adsorption on the concentration profile of the solute inside the pore becomes evident: adsorption starts at the pore entrance region making, for the first instances, the solute concentration to decrease along the membrane depth. In fact, the curve concavity ends up to be

reverted in those instances compared to when steady-state is reached. Then, adsorption spreads out along the membrane depth and, with time, the profile shape approaches that without adsorption.

When adsorption occurs at lower pressures (5 bar, Figure 6 A and E), the hormone concentration reduces considerably along the pore length at the beginning of the experiment, particularly downstream the entrance region. This means high adsorption rates at the pore entrance region in the beginning of permeation.

A higher pressure originates higher concentrations along the pore as can be seen by comparing Figure 6 B and F with Figure 6 A and E, therefore yielding more adsorption. This trend is particularly noticeable at the pore centre and exit and is a consequence of the higher concentration polarisation yielded by higher pressures.

For the highest pressure (15 bar, Figure 6 B and F), convection increases importance: the profile shifts from linear (diffusion-dominated transport) to curve (convection-dominated transport) showing that convection plays a role in the transport of solutes by NF membranes at high pressures. Although present at all instances in Figure 6 B and F, this effect of the convective transport is particularly noticeable when steady-state is approached.

There is a difference in the amount partitioned into the membrane of E1 compared to E2 (*e.g.* Figure 6 A and E): λ is closer to 1 for E2 (λ_{E2}=0.950), compared to E1 (λ_{E1}=0.936) and therefore partitions less inside the pore (equation 8b). E1 is therefore likely to adsorb more because the concentrations inside the membrane are higher (Figure 6).

Interestingly, the concentration of E1 and E2 in the results for the NF 270 membrane at the pore exit are very similar when reaching steady-state, despite the higher permeate concentrations obtained for E2 compared to E1 [13] that were used as boundary condition values for the predictions. This is caused by the small differences in the molecule size of E1 and E2 (Table 3). The closer the solute size is to the pore size, as is the case of E2 compared to E1, the smaller the partition coefficient Φ' will be and therefore, the smaller the concentration inside the membrane on the permeate side will be.

4.4. Model Prediction Results Comparison with Experimental Data

The model predicted mass adsorbed is compared with the corresponding experimental data for several experimental conditions for E1 and E2 (see Figure 7). The model predicts well the total mass of hormone adsorbed in the NF membranes when the hydrodynamic model considers both transient surface and internal sorption.

E1 membrane surface adsorption in the absence of applied pressure (*i.e.* no permeate production) was determined in the cross-flow system as 24 ng. In comparison, the model surface

adsorption for the same hormone at 5 bar gave a prediction of 32 ng compared to a total adsorption of 50 ng, indicating the close estimated value for surface adsorption given by the model. The predicted value by the model at 5 bar is however higher than when no pressure was applied *(i.e.* 24 ng). This is expected because at 5 bar the membrane surface is subjected to a higher concentration, *i.e.* the concentration at the membrane surface due to polarisation (around 125 $ng.L^{-1}$) compared to 100 $ng.L^{-1}$ when no pressure is applied.

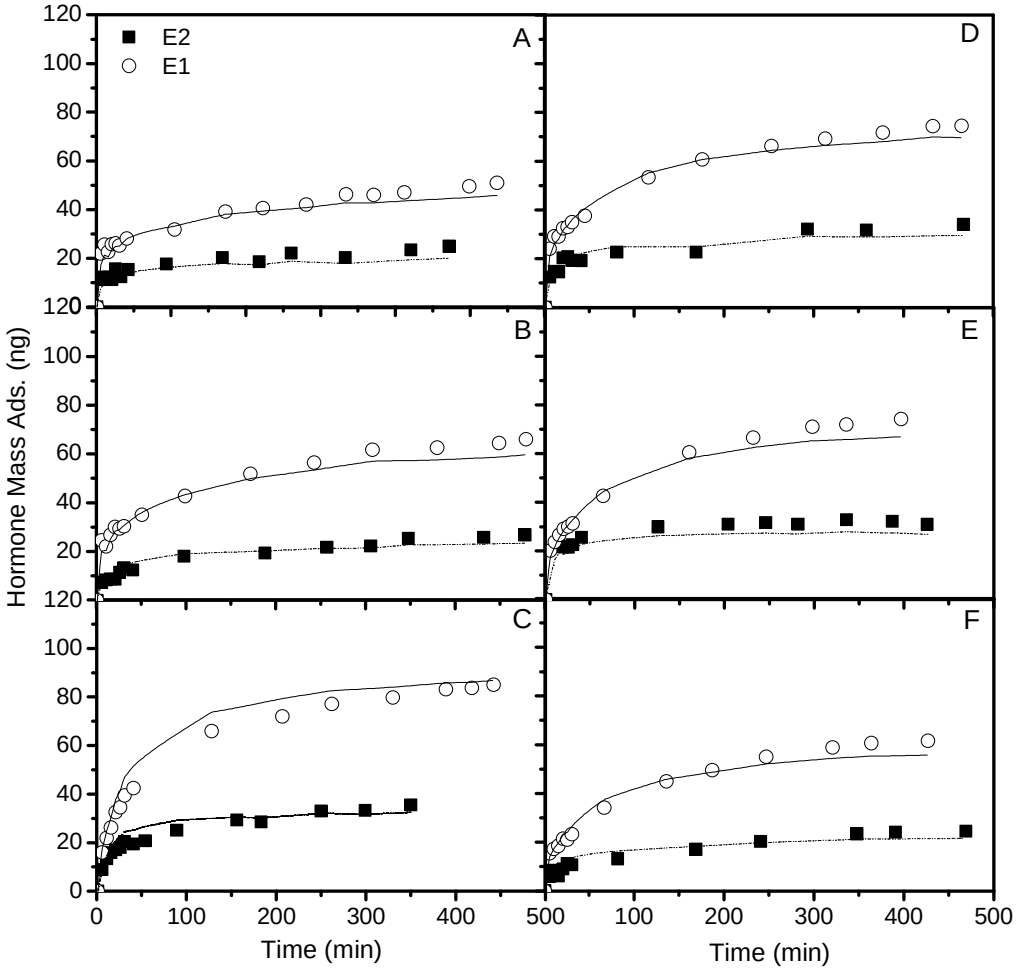

Figure 7 Comparison between experimental and model results of the E1 and E2 mass adsorbed (C_{feed}=100 $ng.L^{-1}$, T=24°C, pH 7): Re_h=427 A) P=5bar, B) P=8 bar, C) P=15 bar; P=11 bar D) Re_h=570, E) Re_h=855, F) Re_h=998

As can be seen in Figure 7, E1 adsorbs at least twice as much mass as E2 for the same filtration conditions and the same membrane. When E1 adsorption in static mode is compared to E2, a higher adsorption of E1 onto the membrane is obtained (Figure 8). However, the difference in adsorption between E1 and E2 in static mode is only 20% which cannot explain the differences obtained in filtration mode. It is however explained by the much higher partitioning of E1 inside the

pore compared to E2. This example illustrates well how similar molecules can behave differently when one partitions more inside the membrane pore.

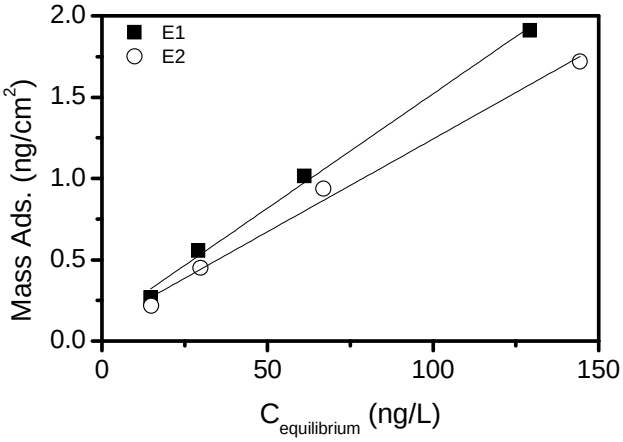

Figure 8 Static isotherm experiments for E1 and E2 and the NF 270 membrane (C_{feed}=25, 50, 100 and 200 ng.L^{-1}, T=24°C, 200 rpm)

Because E1 adsorbs more than E2 this causes more pronounced changes in the time-varying profiles of E1 (Figure 6 A and B) than those observed for E2 (Figure 6 E and F). These differences are more noticeable, as expected, at higher pressures, since larger concentration polarisation occurs.

The effect of adsorption onto NF membranes will not be negligible in real applications. The NF 200 membrane from Dow Filmtec, which has a similar MWCO (300 Da [42]) than the NF270 membrane (200 Da [13]), is used in the Méry-Sur-Oise plant in Paris. This plant started off working at 10 bar pressure in 1999, but due to fouling has now increased to 17 bar [43] so the effect of adsorption at these pressures for a feed concentration of 100 ng.L^{-1} will be significant (~1.5 ng.cm^{-2} for E1 and 0.7 ng.cm^{-2} for E2) and retentions can be lower than 70% once saturation is reached [13].

The impact of adsorption on other membranes will depend on their structure, as shown by the developed model: for tight RO membranes with small porosity the impact is expected to be small, as partitioning inside the membrane is reduced and adsorption will be low. This was shown with the BW30 membrane in Part A of the paper. For a tight membrane with high porosity however, such as the NF90 membrane (part A of the paper) adsorption will be higher, as there is more area to adsorb onto. However, for looser membranes with high porosity, like the TFC-SR2 membranes, adsorption will be much higher due to the higher partitioning inside the pore and a thicker active layer, *i.e.* more internal surface area for adsorption.

5 Conclusions

Hormones partition inside the NF membrane pore, adsorb onto NF polymeric membranes and have a lower retention than would be expected by purely steric interactions. The relationship between solute and pore size is important. The higher r_s/r_p is the better the removal will be by steric exclusion. However, this is not the only factor playing a role in the removal of trace contaminants by NF membranes. The interaction with the membrane polymer may overcome this steric exclusion factor leading to a higher partitioning inside the membrane and hence, higher rates of adsorption. The lower the interaction of trace contaminants with the membrane (Φ') the less will their concentration partition inside the membrane be and, therefore, less will adsorb in the pores. This has an impact on the design of membrane materials. On the other hand, the more internal surface area the membrane has, the more will adsorb in it. The adsorbed contaminants inside the membrane can desorb if there are changes in the feed conditions, causing more permeation through the membrane, decreasing the membrane capacity in retaining adsorbing compounds.

A new model taking into account transient adsorption inside the membrane polymeric active layer was developed allowing understanding the different mechanisms taking place in the transport of these inside the membrane pores and how these depend on the operating conditions. Despite much debate on the occurrence of a convective term in transport of solutes by NF membranes, transport by convection and diffusion described well the transport of adsorbing hormones through NF pores. This term was especially pronounced at pressures higher than 11 bar, commonly used pressure in NF.

In order to develop a fully predictive model, the parameter X that was obtained through fitting with the feed concentration experiments needs to be obtained independently. However, this model clearly shows how the membrane structure and different filtration conditions influence the adsorption on the NF membrane. This is useful in the design of new membrane materials and membrane structures in order to either avoid or enhance adsorption, depending on the application required.

Further attention needs to be taken when studies of adsorbing compounds are carried out. As previously mentioned, misleading conclusions can be taken from studies with the transport of adsorbing trace contaminants in unsaturated membranes, because while adsorption occurs, the permeate concentration will be low for highly adsorbing contaminants such as E1 with the NF 270. These results might lead to the conclusion of a diffusion-dominated transport, when in fact transport

of adsorbing hormones through NF membranes are well described by convective and diffusive mechanisms as is the case for the membranes at pressures higher than 11 bar.

The model developed does not take into account interactions that might occur in real-life applications, such as hormone interaction with natural-organic matter, with a fouling layer on the membrane surface, amongst others. The developed model aims at understanding the fundamental mechanisms of transport of single compounds that adsorb onto NF membranes. The model can however be extended in the future in order to take into account other interactions through, for example, the inclusion of a source term that can include as many mechanisms/interactions as necessary, namely hormone-organic matter interactions.

Acknowledgments

We would like to thank the University of Edinburgh for the studentship and project funding provided to Andrea Semiao, Dow Filmtech for providing the membrane samples. We would further like to thank Dr. Chris McDermott (University of Edinburgh, UK), Dr. Ben Corry (University of Western Australia, Australia), Professor Elimelech and his group (Yale University, USA), Professor Melin (Aachen Unversity, Germany), Dr. Freger and Dr. Ben-David (Ben Gurion University of the Negev, Israel) and Professor Crespo (Universidade Nova de Lisboa, Portugal) for their useful discussions on the modelling work at the University of Edinburgh and during the GRC 2010 conference in New London, USA.

A very special thank you is given to Prof. Polizzi (Universita Ca' Foscari Venezia, Italy) for his TEM measurements of several membranes for the determination of the active layer thickness of the NF 270 membrane.

References

[1] M. Auriol, Y. Filali-Meknassi, R.D. Tyagi, C.D. Adams, R.Y. Surampalli, Endocrine disrupting compounds removal from wastewater, a new challenge, PROCESS BIOCHEM, 41 (2006) 525-539.
[2] J.P. Sumpter, A.C. Johnson, Lessons from endocrine disruption and their application to other issues concerning trace organics in the aquatic environment, Environ. Sci. Technol., 39 (2005) 4321-4332.
[3] S.K. Khanal, B. Xie, M.L. Thompson, S. Sung, S.-K. Ong, J. van Leeuwen, Fate, transport, and biodegradation of natural estrogens in the environment and engineered systems, Environ. Sci. Technol., 40 (2006) 6537-6546.
[4] D.W. Kolpin, E.T. Furlong, M.T. Meyer, E.M. Thurman, S.D. Zaugg, L.B. Barber, H.T. Buxton, Pharmaceuticals, hormones, and other organic wastewater contaminants in U.S. streams, 1999-2000: a national reconnaissance, Environ. Sci. Technol., 36 (2002) 1202-1211.
[5] J.P. Sumpter, Endocrine disrupters in the aquatic environment: an overview, Acta Hydrochim. Hydrobiol., 33 (2005) 9-16.
[6] W.R. Bowen, H. Mukhtar, Characterisation and prediction of separation performance of nanofiltration membranes, J. Membr. Sci., 112 (1996) 263-274.
[7] W.R. Bowen, A.W. Mohammad, N. Hilal, Characterisation of nanofiltration membranes for predictive purposes - use of salts, uncharged solutes and atomic force microscopy, J. Membr. Sci., 126 (1997) 91-105.
[8] C. Combe, C. Guizard, P. Aimar, V. Sanchez, Experimental determination of four characteristics used to predict the retention of a ceramic nanofiltration membrane, J. Membr. Sci., 129 (1997) 147-160.
[9] K. Kimura, G. Amy, J.E. Drewes, T. Heberer, T.-U. Kim, Y. Watanabe, Rejection of organic micropollutants (disinfection by-products, endocrine disrupting compounds, and pharmaceutically active compounds) by NF/RO membranes, J. Membr. Sci., 227 (2003) 113-121.
[10] B. Van der Bruggen, J. Schaep, D. Wilms, C. Vandecasteele, Influence of molecular size, polarity and charge on the retention of organic molecules by nanofiltration, J. Membr. Sci., 156 (1999) 29-41.
[11] D. Libotean, J. Giralt, R. Rallo, Y. Cohen, F. Giralt, H.F. Ridgway, G. Rodriguez, D. Phipps, Organic compounds passage through RO membranes, J. Membr. Sci., 313 (2008) 23-43.
[12] A.I. Schäfer, I. Akanyeti, A.J.C. Semião, Micropollutant sorption to membrane polymers: a review of mechanisms for estrogens, Adv Colloid Interfac, 164 (2011) 100-117.
[13] A.J.C. Semião, A.I. Schäfer, Estrogenic micropollutant adsorption dynamics onto nanofiltration membranes, J. Membr. Sci., 381 (2011) 132-141.
[14] A.R.D. Verliefde, E.R. Cornelissen, S.G.J. Heijman, E.M.V. Hoek, G.L. Amy, B.V.d. Bruggen, J.C. van Dijk, Influence of solute-membrane affinity on rejection of uncharged organic solutes by nanofiltration membranes, Environ. Sci. Technol., 43 (2009) 2400-2406.
[15] L.D. Nghiem, A.I. Schäfer, M. Elimelech, Removal of natural hormones by nanofiltration membranes: measurement, modeling, and mechanisms, Environ. Sci. Technol., 38 (2004) 1888-1896.
[16] L.D. Nghiem, A.I. Schäfer, M. Elimelech, Nanofiltration of hormone mimicking trace organic contaminants, Sep. Sci. Technol., 40 (2005) 2633-2649.
[17] L.D. Nghiem, A.I. Schäfer, Adsorption and transport of trace contaminant estrone in NF/RO membranes, Environ. Eng. Sci., 19 (2002) 441-451.
[18] A.I. Schäfer, L.D. Nghiem, T.D. Waite, Removal of the natural hormone estrone from aqueous solutions using nanofiltration and reverse osmosis, Environ. Sci. Technol., 37 (2003) 182-188.
[19] E.A. McCallum, H. Hyung, T.A. Do, C.-H. Huang, J.-H. Kim, Adsorption, desorption, and steady-state removal of 17β-estradiol by nanofiltration membranes, J. Membr. Sci., 319 (2008) 38-43.

[20] L.D. Nghiem, A.I. Schäfer, Critical risk points of nanofiltration and reverse osmosis processes in water recycling applications, Desalination, 187 (2006) 303-312.
[21] K.M. Agbekodo, B. Legube, S. Dard, Atrazine and simazine removal mechanisms by nanofiltration: influence of natural organic matter concentration, Water Res., 30 (1996) 2535-2542.
[22] E. Steinle-Darling, E. Litwiller, M. Reinhard, Effects of sorption on the rejection of trace organic contaminants during nanofiltration, Environ. Sci. Technol., 44 (2010) 2592-2598.
[23] V. Yangali-Quintanilla, A. Sadmani, M. McConville, M. Kennedy, G. Amy, A QSAR model for predicting rejection of emerging contaminants (pharmaceuticals, endocrine disruptors) by nanofiltration membranes, Water Res., 44 (2010) 373-384.
[24] V. Yangali-Quintanilla, A. Verliefde, T.U. Kim, A. Sadmani, M. Kennedy, G. Amy, Artificial neural network models based on QSAR for predicting rejection of neutral organic compounds by polyamide nanofiltration and reverse osmosis membranes, J. Membr. Sci., 342 (2009) 251-262.
[25] E.R. Cornelissen, J. Verdouw, A.J. Gijsbertsen-Abrahamse, J.A.M.H. Hofman, A nanofiltration retention model for trace contaminants in drinking water sources, Desalination, 178 (2005) 179-192.
[26] A.R.D. Verliefde, E.R. Cornelissen, S.G.J. Heijman, J.Q.J.C. Verberk, G.L. Amy, B. Van der Bruggen, J.C. van Dijk, Construction and validation of a full-scale model for rejection of organic micropollutants by NF membranes, J. Membr. Sci., 339 (2009) 10-20.
[27] T.-U. Kim, J.E. Drewes, R. Scott Summers, G.L. Amy, Solute transport model for trace organic neutral and charged compounds through nanofiltration and reverse osmosis membranes, Water Res., 41 (2007) 3977-3988.
[28] M.E. Williams, J.A. Hestekin, C.N. Smothers, D. Bhattacharyya, Separation of organic pollutants by reverse osmosis and nanofiltration membranes: mathematical models and experimental verification, Ind. Eng. Chem. Res., 38 (1999) 3683-3695.
[29] L. Braeken, B. Van der Bruggen, C. Vandecasteele, Flux decline in nanofiltration due to adsorption of dissolved organic compounds: model prediction of time dependency, J. Phys. Chem. B, 110 (2006) 2957-2962.
[30] A. Ben-David, S. Bason, J. Jopp, Y. Oren, V. Freger, Partitioning of organic solutes between water and polyamide layer of RO and NF membranes: correlation to rejection, J. Membr. Sci., 281 (2006) 480-490.
[31] W.M. Deen, Hindered transport of large molecules in liquid-filled pores, AlChE J., 33 (1987) 1409-1425.
[32] K. Kosutic, L. Kastelan-Kunst, B. Kunst, Porosity of some commercial reverse osmosis and nanofiltration polyamide thin-film composite membranes, J. Membr. Sci., 168 (2000) 101-108.
[33] P. Grathwohl, Diffusion in natural porous media - contaminant transport, sorption/desorption and dissolution kinetics, Kluwer Academic Publishers, Dordrecht, 1998.
[34] G.S. Committee, G.R. Forum, N.R. Council, Groundwater Contamination, National Academy Press Washington D.C., 1984.
[35] C.W. Fetter, Contaminant Hydrogeology, Prentice-Hall, Upper Saddle River, 1992.
[36] R.H. Pletcher, W.J. Mincowycz, E.M. Sparrow, G.E. Schneider, Overview of Basic Numerical Methods, in: W.J. Mincowycz, E.M. Sparrow, G.E. Schneider, R.H. Pletcher (Eds.) Handbook of Numerical Heat Transfer, John Wiley & Sons, New York, 1988, pp. 1-88.
[37] T.W. Kao, C. Park, Experimental investigations of the stability of channel flows. Part 1. Flow of a single liquid in a rectangular channel, J FLUID MECH, 43 (1970) 145-164.
[38] V.C. Patel, M.R. Head, Some observations on skin friction and velocity profiles in fully developed pipe and channel flows, J FLUID MECH, 38 (1969) 181-201.
[39] F.M. White, Fluid Mechanics, International Student Edition ed., McGraw-Hill, Tokyo, London, 1979.
[40] E. Worch, Eine neue Gleichung zur Berechnung von Diffusionskoeffizienten gelöster Stoffe, vom Wasser, 81 (1993) 289-297.
[41] S. Lee, G. Amy, J. Cho, Applicability of Sherwood correlations for natural organic matter (NOM) transport in nanofiltration (NF) membranes, J. Membr. Sci., 240 (2004) 49-65.

[42] P. Xu, J.E. Drewes, T.-U. Kim, C. Bellona, G. Amy, Effect of membrane fouling on transport of organic contaminants in NF/RO membrane applications, J. Membr. Sci., 279 (2006) 165-175.
[43] A. Houari, D. Seyer, F. Couquard, K. Kecili, C. Démocrate, V. Heim, P.D. Martino, Characterization of the biofouling and cleaning efficiency of nanofiltration membranes, Biofouling, 26 (2009) 15-21.

List of Tables

List of Figures